



Wind Farm Dispatch Control for Demand Tracking and Minimized Fatigue

Juelsgaard, Morten; Schiøler, Henrik; Leth, John-Josef

Published in:
8th IFAC Symposium on Power Plant and Power System Control

DOI (link to publication from Publisher):
[10.3182/20120902-4-FR-2032.00068](https://doi.org/10.3182/20120902-4-FR-2032.00068)

Publication date:
2012

Document Version
Early version, also known as pre-print

[Link to publication from Aalborg University](#)

Citation for published version (APA):
Juelsgaard, M., Schiøler, H., & Leth, J-J. (2012). Wind Farm Dispatch Control for Demand Tracking and Minimized Fatigue. In *8th IFAC Symposium on Power Plant and Power System Control* (pp. 381-386). Elsevier. I F A C Workshop Series <https://doi.org/10.3182/20120902-4-FR-2032.00068>

General rights

Copyright and moral rights for the publications made accessible in the public portal are retained by the authors and/or other copyright owners and it is a condition of accessing publications that users recognise and abide by the legal requirements associated with these rights.

- Users may download and print one copy of any publication from the public portal for the purpose of private study or research.
- You may not further distribute the material or use it for any profit-making activity or commercial gain
- You may freely distribute the URL identifying the publication in the public portal -

Take down policy

If you believe that this document breaches copyright please contact us at vbn@aub.aau.dk providing details, and we will remove access to the work immediately and investigate your claim.

Wind Farm Dispatch Control for Demand Tracking and Minimized Fatigue

M. Juelsgaard, H. Schiøler and J. Leth

*Dept. of Automation and Control, University of Aalborg, Denmark,
e-mail: {mju, henrik, jjl}@es.aau.dk*

Abstract: This work presents a strategy for dispatching production references to the individual turbines in a wind farm, such that an overall production demand for the farm is obeyed, while the fatigue experienced by the turbines is minimized. Using a turbine fatigue model for simulating the aging across the farm, we show that a 17 % reduction of the turbine aging can be obtained compared to a commonly employed industrial dispatcher, without degrading the power demand tracking.

Keywords: Wind farms; Power distribution; Load dispatching; Fatigue minimization; Convex optimisation; Predictive control;

1. INTRODUCTION

For a number of years, the Danish use of wind turbines for electrical power generation has increased, and is further expected to increase in the future (Energinet.dk [2010a]). It is common to operate wind turbines and wind farms in a way that maximizes power production, however as more wind power is implemented, this production scheme will not persist to be feasible (Behnke [2011]). With significant penetration of wind energy, it is paramount that wind turbines participate in balancing the electrical grid, in order to maintain a steady grid frequency.

Recent new requirements for ancillary services of wind power plants, have been presented (Energinet.dk [2010b]). Turbines are for example required to be capable of operating in Δ -mode, where a requested production reserve must be maintained, with respect to the available power. Situations where a wind farm operates in Δ -mode, yields the possibility of dispatching production references for the individual turbines, obeying not only the overall production demand, but also reducing the experienced fatigue.

This constitutes the focus of our work, where we employ a turbine model for simulating the power production and fatigue experienced by an individual turbine. We use this as a vantage point for obtaining a dispatch strategy for power references across the wind farm. This strategy dispatches references, such that both the overall production demand is obeyed, and the fatigue is minimized.

In the following, we describe the employed turbine model, and how it is expanded to cover an entire farm. This is done in Section 2, whereafter Section 3 formulates the dispatching problem. We demonstrate that the problem is non-convex, and employ a two-step strategy where we first simplify the problem, and afterwards find an approximate solution. This two-step strategy is described in Section 4 and 5. Section 6 presents a numerical example, before Section 7 summarizes our results, and presents suggestions for future work.

2. MODELING

Below we outline the elements of the model used to simulate a wind turbine. We then present the turbine fatigue model, and finally explain how we extend the modeling of a single turbine, to an entire farm.

2.1 Turbine Model

The turbine model consists of the blocks illustrated in Fig. 1. We give an overall explanation of the model below, however as turbine modeling is not part of this work, the analysis is limited.

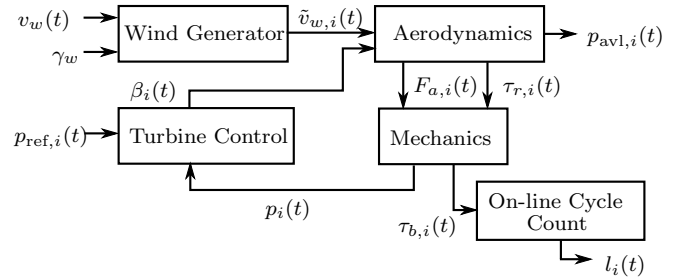


Fig. 1. Block diagram of the wind turbine model.

Wind Generation From a provided average wind speed $v_w(t) \in \mathbf{R}$, where $t \in [0; \infty)$ denotes time, and a turbulence intensity $\gamma_w \in \mathbf{R}$, the wind generator provides a stochastic wind $\tilde{v}_{w,i}(t) \in \mathbf{R}$ as output. Here $i = 1, \dots, n$ refers to the turbines in the farm. The average wind speed $v_w(t)$ is assumed equal for all turbines, but the stochastic elements of the wind, are statistically independent for the turbines, hence the subscript i . Over time $v_w(t)$ can change, however changes would typically be very slow, and related to meteorological weather dynamics. Changes in $\tilde{v}_{w,i}(t)$ are fast, and related to the turbulence in the wind. We will return to this in Section 2.3.

The wind field is generated using the wind turbine blockset for Matlab Simulink (Iov et al. [2004]). In Fig. 2 we have presented a sample wind field with constant $v_w(t)$.

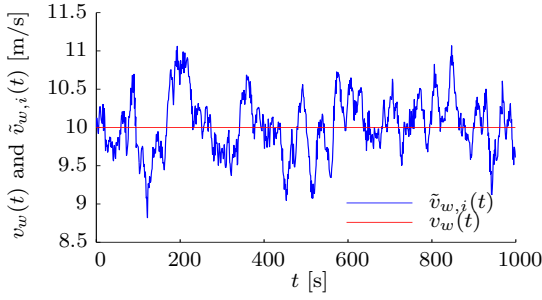


Fig. 2. Sample of a wind field $\tilde{v}_{w,i}(t)$ with $v_w(t) = 10$ m/s and $\gamma_w = 6$ %.

Since the wind field is the source of the available power, the variations of the wind field, both fast and slow, can be translated to variations in the available power.

Turbine Controller The turbine controller regulates the pitch of the blades $\beta_i(t) \in \mathbf{R}$, in order for the produced power $p_i(t) \in \mathbf{R}$ to track the provided reference $p_{\text{ref},i}(t) \in \mathbf{R}$. The reference is provided by a dispatcher, as part of the farm controller. The design of this reference is the focus of this work.

Aerodynamics Based on the incoming wind field $\tilde{v}_{w,i}(t)$, and the pitching of the turbine blades, the axial thrust force $F_{a,i}(t) \in \mathbf{R}$ and the rotational torque $\tau_{r,i}(t) \in \mathbf{R}$ of the rotor, are calculated as well as the available power in the wind, $p_{\text{avl},i}(t) \in \mathbf{R}$. The aerodynamic calculations are similar to those presented in the literature (Burton et al. [2001], Stiebler [2008]).

Mechanics From the force and torque calculated by the aerodynamic block, the dynamic behavior of the turbine tower and drive train can be modeled. The axial thrust $F_{a,i}(t)$ is translated to a fore-aft bending moment $\tau_{b,i}(t) \in \mathbf{R}$, causing displacement of the turbine nacelle, and a swaying motion of the tower. The rotational torque $\tau_{r,i}(t)$ is translated to a produced power $p_i(t) \in \mathbf{R}$, using the drive train model.

On-line Cycle Count The nacelle deflection and tower swaying caused by the bending moment $\tau_{b,i}(t)$, is used by the On-line Cycle Count (OCC), in order to calculate the age $l_i(t) \in \mathbf{R}$ of the turbine. Here the age is a measure of the wear and tear the turbine has experienced until time t . The calculation of the age resembles the rain flow counting algorithm, as described for instance by Downing and Socie [1982]. It depends on both the number and amplitude of the deflections made by the tower. We will further explore how to model the aging in the following section.

2.2 Fatigue Model

We define the fatigue rate of a turbine, as the change in age over time. By running a number of simulations with the above model, sweeping for a range of power references, we obtain a mapping between $p_{\text{ref},i}(t)$, and the fatigue rate $f_i(p_{\text{ref},i}) \in \mathbf{R}$. We present this in Fig. 3 for a number of average wind speeds.

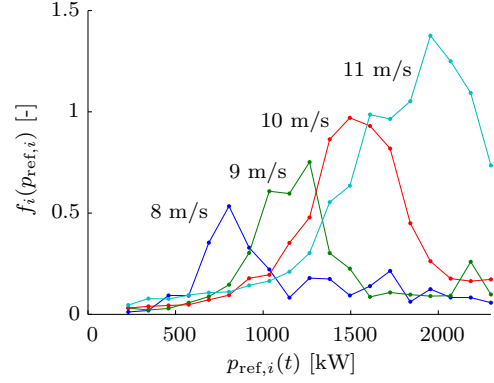


Fig. 3. The fatigue rate $f_i(p_{\text{ref},i})$ as a function of production reference $p_{\text{ref},i}(t)$, for $v_w(t) = 8, 9, 10, 11$ m/s and $\gamma_w = 6$ %.

As illustrated by Fig. 3, the fatigue rate only increases up to a certain point. Increasing $p_{\text{ref},i}(t)$ further yields a decrease in fatigue rate. This is related to the pitching of the turbine blades. In order for the turbine to increase power production, it increases the torque around the rotor axis. This corresponds to reducing the pitch angle of the blades, in order to increase the aerodynamic lift (Burton et al. [2001], Stiebler [2008]). Assuming a constant wind field, this entails that whenever the power reference increases, the pitch decreases.

However, as the wind field is not constant, the pitch needs to track the wind variations, in order to maintain a constant power production. These pitch variations causes the axial thrust force experienced across the swept area, to fluctuate, which increases the fatigue rate.

This entails that when the power reference for a turbine increases from a lower to a higher value, the pitch generally shifts to a lower average value. However, the pitch $\beta_i(t)$, is truncated by a lower limit β_{min} , which at some point causes the pitch actuator to saturate as illustrated in Fig. 4. As this lower limit causes the pitch variations to decrease, the variations in axial thrust force, and thereby the fatigue rate also decreases. This explains the reduction in fatigue rate for large references in Fig. 3.

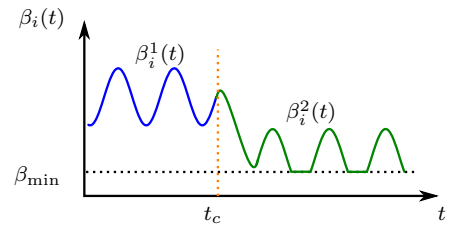


Fig. 4. At $t = t_c$, the turbine receives an increased power reference and changes the pitch from $\beta_i^1(t)$ to $\beta_i^2(t)$, which is truncated by actuator saturation.

The decrease in fatigue rate for large power references, only exists in cases where the available power does not exceed the rated power $p_{\text{max}} \in \mathbf{R}$, in that if $p_{\text{max}} < p_{\text{avl},i}(t)$, for all t , the fatigue rate would only increase with increased power references. We therefore require that $p_{\text{avl},i}(t) \leq p_{\text{max}}$.

2.3 Farm Model

The discussions in Section 2.1 and 2.2 only relates to the modeling of a single turbine. In this work, we model a farm as a collection of individual turbines, disregarding any inter-turbine correlations, such as increased turbulence or reduced wind speed. We assume that the wind field at each turbine has the same fundamental characteristics, as given by $v_w(t)$ and γ_w , but that the stochastic components of each wind field are uncorrelated.

3. PROBLEM FORMULATION

We consider a turbine farm, consisting of n turbines. The farm is required to track a power demand $p_{\text{dem}}(t) \in \mathbf{R}$, within an allowed deviation ϵ . We assume that this demand is known in advance, for instance as a result of the power market, and auctions at the power exchange. We also assume that $p_{\text{dem}}(t) < \sum_{i=1}^n p_{\text{avl},i}(t)$, *i.e.* the farm operates in Δ -mode.

In order for the farm to track $p_{\text{dem}}(t)$, a production reference $p_{\text{ref},i}(t) \in \mathbf{R}$, $i = 1, \dots, n$, is dispatched to each turbine in the farm. These references should obey

$$\left| \sum_{i=1}^n p_{\text{ref},i}(t) - p_{\text{dem}}(t) \right| \leq \epsilon.$$

The production references are limited above and below, where the lower limit $p_{\text{min}} \in \mathbf{R}$ would typically be zero. With respect to the optimization, the upper limit is dictated by both the rated power of the turbine $p_{\text{max}} \in \mathbf{R}$, as well as the available power $p_{\text{avl},i}(t)$. In general, $p_{\text{ref},i}(t)$ may exceed $p_{\text{avl},i}(t)$, however we will not allow this in optimization problems, as applying references exceeding the available power, would yield a divergence between the reference, and the feasible production of the turbine. From this we have

$$p_{\text{min}} \leq p_{\text{ref},i}(t) \leq \min\{p_{\text{max}}, p_{\text{avl},i}(t)\}, \quad (1)$$

for $i = 1, \dots, n$.

The power references are further subject to slew-rate constraints such that

$$\left| \frac{d}{dt} p_{\text{ref},i}(t) \right| \leq \Delta p_{\text{max}}, \quad (2)$$

for $i = 1, \dots, n$. Collecting the above bounding and slew-rate constraints in the set \mathcal{P} , (1) and (2), can be expressed as $p_{\text{ref},i}(t) \in \mathcal{P}$. We refer to the collection of power references, as a power distribution across the wind farm.

To any reference $p_{\text{ref},i}(t)$, is related a mechanical stress, given by the fatigue rate $f_i(p_{\text{ref},i}) > 0$, as illustrated in Fig. 3. It should be noted that Fig. 3 was made using constant references, *i.e.* $p_{\text{ref},i}(t) = c$, with $0 \leq c \leq p_{\text{max}}$, but the mechanical stress is also affected by changes in the power reference. We apply an approximated age function $l_i(t)$ given by

$$l_i(t) = \int_0^t f_i(p_{\text{ref},i}) + a_i \left(\frac{dp_{\text{ref},i}(t)}{dt} \right)^2 dt$$

where $l_i(t) \in \mathbf{R}$ and $a_i \in \mathbf{R}$. From this, the task of arranging the power distribution, minimizing the fatigue of each turbine, is expressed as

$$\begin{aligned} & \text{minimize} \quad \sum_{i=1}^n \int_0^T f_i(p_{\text{ref},i}) + a_i \left(\frac{d}{dt} p_{\text{ref},i}(t) \right)^2 dt \\ & \text{subject to} \quad \left| \sum_{i=1}^n p_{\text{ref},i}(t) - p_{\text{dem}}(t) \right| \leq \epsilon \\ & \quad p_{\text{ref}}(t) \in \mathcal{P}, \end{aligned} \quad (3)$$

with variable $p_{\text{ref}}(t) = [p_{\text{ref},1}(t), \dots, p_{\text{ref},n}(t)] \in \mathbf{R}^n$, for $0 \leq t \leq T$.

Note that this problem is non-convex (Boyd and Vandenberghe [2004]), as the fatigue rate $f_i(p_{\text{ref},i})$ is not a convex function. As mentioned in the introduction, we employ a two-step strategy for dealing with this. This strategy involves first finding an operating point, around which we then arrange a convex approximation to (3).

4. OFF-LINE DISTRIBUTION

The first step of our dispatch strategy, is to find the optimal operating point. This operating point will only have to be found as an initialization, whenever $p_{\text{dem}}(t)$ changes, and afterwards be updated during runtime. For this reason, we refer to the following as an off-line distribution. Our approach will be to initially design the off-line distribution as the optimal average production of the turbines, without considerations to the specific transient variations of the available power for each turbine.

In Fig. 3 we presented the fatigue curve, obtained by running a number of simulations with a constant power reference. However, as we explained, we will in general assume only that $p_{\text{avl},i}(t) \leq p_{\text{max}}$, so at some points we might apply references exceeding the available power, and we therefore have a mismatch between the applied reference and obtainable production. Therefore, in order to gain insight in the fatigue rate as a function of the produced power, we define a mapping between the applied reference $p_{\text{ref},i}(t)$, and the average production $\bar{p}_i(p_{\text{ref},i}) \in \mathbf{R}$, for constant references over time. We obtain the average produced power by

$$\bar{p}_i(p_{\text{ref},i}) = \frac{1}{T} \int_0^T \min\{p_{\text{ref},i}, p_{\text{avl},i}(t)\} dt, \quad (4)$$

where we have omitted the time dependence on $p_{\text{ref},i}$, as it is assumed constant over time. Above, T is chosen to be large enough to consider \bar{p}_i as a valid measure of the average production, under a given constant reference.

Using the mapping (4), we transform the data from Fig. 3 to depict the fatigue rate as a function of average production. This is presented in Fig. 5 for $v_w(t) = 10$ m/s. The task of the off-line distribution is now to arrange a distribution for the average production for turbines, minimizing the farm fatigue, *i.e.*

$$\begin{aligned} & \text{minimize} \quad \sum_{i=1}^n f_i(\bar{p}_i) \\ & \text{subject to} \quad \left| \sum_{i=1}^n \bar{p}_i - p_{\text{dem}} \right| \leq \epsilon \\ & \quad 0 \leq \bar{p} \leq \bar{p}_{\text{max}}, \end{aligned} \quad (5)$$

with variable $\bar{p} = [\bar{p}_1, \dots, \bar{p}_n]^T \in \mathbf{R}^n$, where we have omitted the dependence on $p_{\text{ref},i}$ in the notation. We denote the maximum average production by $\bar{p}_{\text{max}} \in \mathbf{R}$, as indicated in Fig. 5. The solution to (5), dictates what each turbine should produce on average.

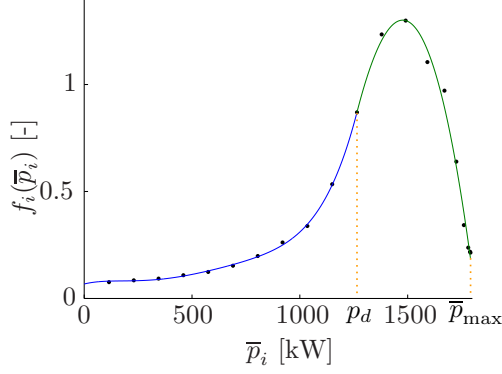


Fig. 5. The fatigue rate as a function of average production. The solid curve illustrates convex and concave approximations around $\bar{p}_i = p_d$.

We solve (5) by splitting Fig. 5 into a right- and a left side around the point p_d . The point p_d is chosen such that the left side of Fig. 5, can be approximated by a convex function, and the right side by a concave. Using these approximations, we divide the task of solving (5) in to 4 sub-problems:

1. Find the number n_l , of left side turbines (LST), where $\bar{p}_i \leq p_d, i = 1, \dots, n_l$ and correspondingly, the number $n_r = n - n_l$, of right side turbines (RST), with $\bar{p}_i > p_d, i = n_l + 1, \dots, n$.
2. Find the optimal right and left side demand, denoted $p_{\text{dem},r}$ and $p_{\text{dem},l}$, that should be produced by the RSTs and LSTs, such that $p_{\text{dem}}(t) = p_{\text{dem},r} + p_{\text{dem},l}$.
3. Find optimal distribution of the left side turbines.
4. Find optimal distribution of the right side turbines.

Right Side Optimality We start with item 4 from the list. Assuming we know n_r and $p_{\text{dem},r}$, the optimal right side distribution solves

$$\begin{aligned} & \text{minimize} \quad \sum_{j=1}^{n_r} f_j(\bar{p}_j) \\ & \text{subject to} \quad \sum_{j=1}^{n_r} \bar{p}_j = p_{\text{dem},r} \\ & \quad \quad \quad p_d \leq \bar{p}_j \leq \bar{p}_{\text{max}}, \end{aligned} \quad (6)$$

with variable $\bar{p}_j, j = 1, \dots, n_r$.

Assuming concavity of the right side in Fig. 5, it can be shown that the solution to (6), is given by (Juelsgaard [2011]):

$$\bar{p}_j = \begin{cases} \bar{p}_{\text{max}}, & j \leq h \\ p_d^+, & j = h + 1, \\ p_d, & j > h + 1 \end{cases} \quad (7)$$

where $h = \lfloor p_{\text{dem},r} / \bar{p}_{\text{max}} \rfloor$, and $p_d^+ = p_{\text{dem},r} - h\bar{p}_{\text{max}} - (n_r - h - 1)p_d$.

Left Side Optimality Assuming that n_l and $p_{\text{dem},l}$ are known, the optimal left side distribution solves

$$\begin{aligned} & \text{minimize} \quad \sum_{s=1}^{n_l} f_s(\bar{p}_s) \\ & \text{subject to} \quad \sum_{s=1}^{n_l} \bar{p}_s = p_{\text{dem},l} \\ & \quad \quad \quad p_{\text{min}} \leq \bar{p}_s \leq p_d. \end{aligned}$$

Assuming convexity of the left side in Fig. 5, it can be shown that the optimal left side distribution is given by (Juelsgaard [2011])

$$\bar{p}_s = \frac{p_{\text{dem},l}}{n_l}, s = 1, \dots, n_l. \quad (8)$$

Optimal Number of Left and Right Turbines We now address item 1 and 2 in the list from before. When deciding n_r and n_l , we require that

$$n = n_l + n_r \quad \text{and} \quad p_{\text{dem}}(t) = p_{\text{dem},l} + p_{\text{dem},r}.$$

This entails that whenever one of either n_l or n_r , and one of either $p_{\text{dem},l}$ or $p_{\text{dem},r}$ has been decided, the optimal off-line power distribution can be found, using the arguments on left- and right side optimality, presented in (7) and (8). Finding the optimal n_r is a finite problem, as there is only finitely many values that n_r can attain. On the other hand, $p_{\text{dem},r}$ is a continuous variable, only constrained by

$$n_r p_d \leq p_{\text{dem},r} \leq n_r \bar{p}_{\text{max}}.$$

Given the arguments in (7) and (8), the optimal off-line distribution is found by solving

$$\begin{aligned} & \text{minimize} \quad hf(\bar{p}_{\text{max}}) + f(p_{\text{dem},r} - h\bar{p}_{\text{max}}) \\ & \quad \quad \quad + (n_r - h - 1)f(p_d) + n_l f(p_{\text{dem},l}/n_l) \\ & \text{subject to} \quad n_l = n - n_r \\ & \quad \quad \quad p_{\text{dem},l} = p_{\text{dem}}(t) - p_{\text{dem},r} \\ & \quad \quad \quad n_r p_d \leq p_{\text{dem},r} \leq n_r \bar{p}_{\text{max}} \\ & \quad \quad \quad h = \lfloor p_{\text{dem},r} / \bar{p}_{\text{max}} \rfloor \end{aligned} \quad (9)$$

with variables $n_r \in \mathbf{R}$ and $p_{\text{dem},r} \in \mathbf{R}$. The cost to minimize in (9), accounts for the fatigue of both right and left side fatigues.

We can approximately solve (9) via exhaustive search, by quantizing the allowed range of $p_{\text{dem},r}$, and then sweeping for all values of n_r , and all quantized values of $p_{\text{dem},r}$. In (9) we have assumed that all turbines operate with the same fatigue curve, which is valid given our prior assumption that the wind fields of each turbine is characterized by the same $v_w(t)$ and γ_w .

5. ON-LINE DISTRIBUTION

The off-line distribution does not explicitly account for the available power of the individual turbine, so in order to obey the deviation limit on $p_{\text{dem}}(t)$, the specific available power at any time, has to be taken into account. This is conducted through an on-line update of the off-line distribution. The on-line distribution is calculated as a solution to a convex approximation of (3), where the off-line distribution from (9) serves as an operating point.

In order to obtain a convex approximation to (3), we create affine approximations of the fatigue curve, around the operating point found in the off-line distribution. We further discretize time in (3), where we limit our optimization scope to a horizon of N steps. This corresponds to a large extend, to the model predictive strategy described by Maciejowski [2000]. The discretized, convex approximation to (3) is described as

$$\begin{aligned} & \text{minimize} \quad \sum_{j=1}^N \sum_{i=1}^n (\tilde{f}_i(p_{\text{ref},i}(k+j))^2 \\ & \quad \quad \quad + \lambda(\Delta p_{\text{ref},i}(k+j))^2) \\ & \text{subject to} \quad \left| \sum_{i=1}^n p_{\text{ref},i}(k+j) - p_{\text{dem}}(k+j) \right| \leq \epsilon \\ & \quad \quad \quad p_{\text{ref}}(k) \in \mathcal{P}, \end{aligned} \quad (10)$$

with variable $p_{\text{ref},i}(k+j)$, $i = 1, \dots, n$ and $j = 1, \dots, N$. Further $\Delta p_{\text{ref},i}(k+j) = p_{\text{ref},i}(k+j) - p_{\text{ref},i}(k+j-1)$. Finally, $\hat{f}_i(p_{\text{ref},i})$ are affine approximations to $f_i(p_{\text{ref},i})$, around the operating point, and $\lambda \in \mathbf{R}$ is a trade-off parameter.

We solve (10) during runtime, and continuously calculate a power distribution for the following N time-steps, where we would make on-line updates of the affine approximations \hat{f}_i . Problem (10) thereby acts as an on-line update of the off-line distribution, where the available power is accounted for, in order to avoid production deficiency by applying references, exceeding the available power.

The on-line update of the power distribution entails that RSTs will produce a power that to some extent follows the available power in the wind, as this yields a smaller fatigue. In order to counteract the power variations that follows from this, the LSTs also needs to produce a varying power, in order for the farm to obey the demand deviation. These variations causes an increased fatigue on the LSTs.

5.1 Swapping

As described, the power balancing performed by the LSTs, entails that these turbines experiences increased fatigue. This means that the LSTs are typically aged faster, and the ages of LSTs and RSTs will therefore drift apart. The effect of this can be shown to decrease, as the farm size increases, given our assumption that the wind fields are uncorrelated for the individual turbines. However, if this drift is not taken into account, a significant difference in age could be obtained, which increases the risk that some turbines break down earlier than others. We avoid this by introducing a swap between the left and right side turbines, meaning that we interchange their operating point with respect to which side of the fatigue curve they operate on. This effectively interchanges their fatigue rates, as illustrated in Fig. 6.

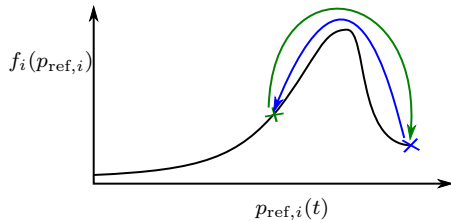


Fig. 6. A swap relocates turbines from one side of the fatigue curve, to the other, in order to interchange their fatigue rate.

It should be noted, that if such swaps are implemented in a full-speed wind field, the turbine tower would experience significant changes in the bending moment, while changing the production to accommodate the new reference. This would yield a significant increase in the age. Therefore, these swaps should only be performed during periods where $v_w(t)$ is low. We illustrate this in the following with a numerical example.

6. NUMERICAL EXAMPLE

Below we present a numerical example, illustrating the benefits from the dispatching method outlined in Section 4

and 5. Initially, we will however describe a commonly employed industrial dispatcher, to which we will compare our results. The comparison dispatcher is similar to the strategy presented in Sørensen et al. [2005] in that a proportional dispatch of the demand is used, however instead of dispatching references as a fraction of the power demand, our comparison dispatcher computes references as an offset to available power of each individual turbine. This is elaborated below.

6.1 Comparison Dispatcher

At any discrete time instance k , the comparison dispatcher arranges a power distribution by

$$p_{\text{ref},i}(k) = p_{\text{avl},i}(k) + \frac{p_{\text{dem}}(k) - \sum_{j=1}^n p_{\text{avl},j}(k)}{n},$$

with $i = 1, \dots, n$. Assuming the farm is capable of producing the demand, this strategy dispatches references as an offset to the available power of the individual turbines, in a way that still obeys the power demand. This dispatching strategy thereby fully accounts for the available power of the turbines, however it does not pay any attention to their fatigue rates.

We will refer to this strategy, as the \mathcal{A} -dispatcher, as it dispatches references relative to available power. Similarly, we refer to the strategy described in Section 4 and 5, as the \mathcal{F} -dispatcher, as it arranges references with respect to the fatigue.

6.2 Example

We consider a farm consisting of $n = 13$ turbines, with a demand of $p_{\text{dem}}(t) = 18,2$ MW, corresponding to an average production reference of 1400 kW. This reference has been chosen, as this corresponds roughly to the peak of the fatigue curve.

We generate wind fields around an average wind speed of $v_w(t) = 10$ m/s, and a turbulence intensity of $\gamma_w = 6$ %, and a simulated time period of 50 hours. We have included 3 periods of low wind speed, where the \mathcal{F} -dispatcher is allowed to perform swaps between right- and left side turbines. In the low wind speed periods we use an average wind speed of $v_w(t) = 5$ m/s. The results from the example are shown in Fig. 7 through 9.

Fig. 7 illustrates the production of each turbine using the two strategies. As can be seen, the \mathcal{F} -dispatcher has turbines producing both close to maximum, as well as turbines producing only little power. This is in order to obtain a reduction in the fatigue rate over the \mathcal{A} -dispatcher, where all turbines produce roughly the same. During the low wind periods, all turbines produce available power, when employing both the \mathcal{A} and \mathcal{F} -dispatcher.

In Fig. 8 the corresponding evolution of the ages are presented for the two strategies. As is evident, the \mathcal{A} -strategy obtains roughly the same fatigue rate on all turbines, whereas \mathcal{F} obtains small fatigue rates on the RSTs, and a slightly larger fatigue rate on the LSTs. However, by implementing swaps during the low wind periods, the \mathcal{F} -dispatcher obtains an aging reduction of roughly 17 % for the oldest turbine, compared to the \mathcal{A} -dispatcher. Extrapolating this to a lifetime of 20 years,

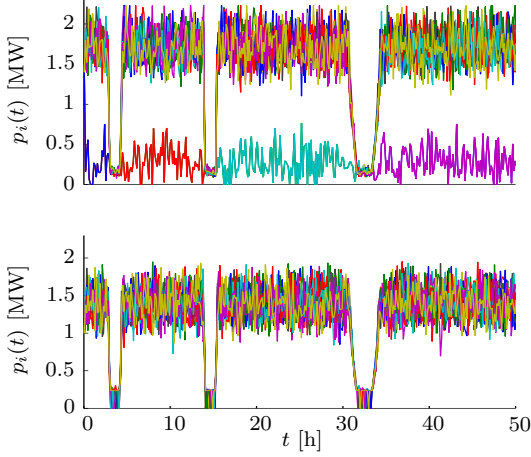


Fig. 7. Turbine power production for the \mathcal{F} -dispatcher (Top), \mathcal{A} -dispatcher (Bottom).

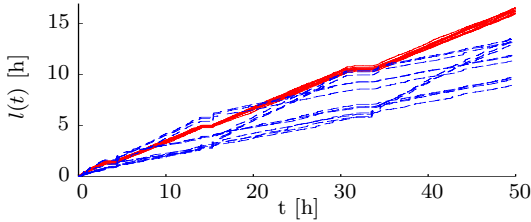


Fig. 8. The age evolution for all turbines in the park, for both the \mathcal{F} -dispatcher (Dashed), and the \mathcal{A} -dispatcher (Solid).

this translates to roughly 3,4 years in difference, between the two dispatching strategies.

The demand tracking for the strategies, is presented in Fig. 9, along with the allowed deviation limits. It is clear that the demand tracking when using the \mathcal{F} -dispatcher, suffers from an increased variation, compared to the \mathcal{A} -dispatcher. This should be expected, as the \mathcal{F} -dispatcher operates closer to the available power, and is therefore affected harder by erroneous estimates of this. However, for the majority of the presented simulation, the optimized dispatcher obeys the demand deviation bounds, though some spikes violates the bounds, throughout the simulation. This is however not an issue related to the dispatching strategy itself, but is rather related to our heuristic way of identifying changes in the average wind speed, in order to reveal low wind periods where swaps can be introduced. By improving the method employed for detecting low wind periods, these spikes could be avoided altogether. Overall, even with increased variation, no significant degradation in the demand tracking is introduced when using the \mathcal{F} -dispatcher.

7. CONCLUSION

This work has presented a model of the fatigue experienced by wind turbines in a wind farm. The model has revealed how the fatigue decreases for large power references. Employing this model, we have obtained a dispatching strategy that tracks a predetermined power demand for the turbine farm, while minimizing the fatigue experienced by the individual turbines.

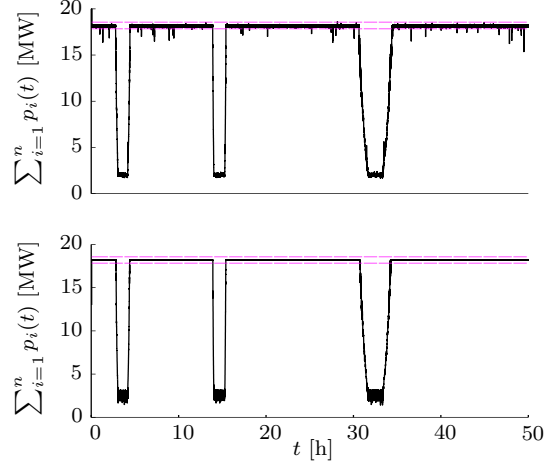


Fig. 9. Demand tracking for the \mathcal{F} -dispatcher (Top), and the \mathcal{A} -dispatcher (Bottom). The dashed, horizontal lines indicate the deviation limits.

Using this dispatch strategy, we have presented simulations, where the numerical results reveal a 17 % decrease in the aging over time, compared to a common industrial dispatching strategy, without experiencing significant degradation in the demand tracking. A practical implementation of our dispatcher, verifying the simulation results, is left as future work.

In this work we have assumed that all turbines in the farm, operate with the same fatigue curve. Future work should investigate how to dispatch power references for turbines with different fatigue curves, *i.e.* turbines operating in wind fields with different characteristics. Similarly, this work has only focused on a single parameterization of the wind field. A suggestion for future work would thereby also entail an implementation accommodating several parameterizations of the wind.

REFERENCES

- K. Behnke. *Power System 2020 - We are building the Smart Grid now*. <http://goo.gl/HJnw1>, 2011. Presented at the 3rd meeting of the danish smart grid network.
- S. P. Boyd and L. Vandenberghe. *Convex optimization*. Cambridge University Press, 2004.
- T. Burton, D. Sharpe, N. Jenkins, and E. Bossanyi. *Wind energy handbook*. Wiley, 2001.
- S. D. Downing and D. F. Socie. Simple rainflow counting algorithms. *International Journal of Fatigue*, 4(1):31–40, 1982.
- Energinet.dk. *Energi 2050 - Udviklingsspor for elsystemet*. www.energinet.dk, 2010a.
- Energinet.dk. *Technical Regulations 3.2.5 for wind power plants with a power output greater than 11 kW*. <http://energinet.dk/>, nov. 2010b.
- F. Iov, A. D. Hansen, P. Sørensen, and F. Blaabjerg. *Wind Turbine Blockset in Matlab/Simulink*, 2004.
- M. Juulsgaard. *Optimal Fatigue Load Distribution in Wind Farms*. Master Thesis, Aalborg University, 2011.
- J. Maciejowski. *Predictive control with constraints*. Prentice Hall, 2000.
- P. Sørensen, A. D. Hansen, K. Thomsen, T. Buhl, P. E. Morthorst, L. H. Nielsen, F. Iov, F. Blaabjerg, H. A. Nielsen, H. Madsen, and M. H. Donohov. Operation and control of large turbines and wind farms. September 2005.
- M. Stiebler. *Wind Energy Systems for Electric Power Generation*. Springer, 2008.